Islamic University Journal of Applied Sciences (IUJAS)
https://journals.iu.edu.sa/jesc

Volume VII, Issue I, 1 July 2025, Pages 149-167

Synergy of (L1, H2, H∞) Norms for Nonlinear Optimal PEMFC Dynamic MIMO Model Reduction using a Novel ANN-BBO Approach

Zohra Touati [1], Slami Saadi [2], Hibat errahmane Benmessaoud [3], Abdelaziz Rabehi [4, *]

[1] Exact Sciences and Informatics Faculty, Djelfa University, Algeria, ztouati@gmail.com

[2] Technology Faculty, Laghouat University, Algeria, s.saadi@univ-djelfa.dz

[3] Exact Sciences and Informatics Faculty, Djelfa University, Algeria, hibaking@gmail.com

[4] Telecommunications and Smart Systems Laboratory, University of Djelfa, PO Box 3117, 17000, Djelfa, Algeria, rab_ehi@hotmail.fr

*Corresponding author: (A. Rabehi), *Email Address*: rab_ehi@hotmail.fr

Abstract

In this work, we present an optimal reduced order nonlinear dynamic model for proton exchange membrane fuel cell (PEMFC) using the minimization of error between original and reduced order models via (L1, H2, H∞) norms synergy optimized with biogeography-based optimization (BBO) Algorithm. The data necessary to form the autoregressive exogenous (ARX) artificial neural network (ANN) model are generated by the simulation of the dynamic model of the nonlinear PEMFC500w differential equations to extract space state matrices values. This approach is compared with Balanced Truncation (BT) model reduction method and illustrated through simulation results.

Keywords: Norms (L_1, H_2, H_∞); ANN; PEMFC; Order reduction; Balanced Truncation; Biogeography-based optimization.

https://doi.org/10.63070/jesc.2025.010
Received 24 March 2025; Revised 28 April 2025; Accepted 14 May 2025.
Available online 25 May 2025.

1. Introduction

Model order reduction intends to decrease the calculation difficulty such as reproduction of significant dynamical and control systems at the same time maintaining major performances of the original system. Specifically, the use of low order models lead to the following desired properties like simple design and analysis, computational advantage and simplicity of simulation. The first technique of model reduction is the model study by state space procedures presented by Davison in 1966 [1]. Moore in 1981designed the theory of balancing, that directed to the well known technique of estimate by unbiased truncation [2]. Though, Moore's advance still endure from stability. Wilson in [3-4] employs an H_2 norm model reduction approach based on the minimization of the integral squared impulse response error among the complete and reduced order models. In 2006,Gugercin et al. [5] suggested an iterative rational Krylov approach (IRKA) for optimal H2 model reduction. In 2010, Bunse-Gerstner et al.[6] proposed an H2 optimal interpolation used for big size discrete dynamical multiple input, multiple output (MIMO) systems. Lately, Panda et al. [7] applied a particle swarm optimization Algorithm to achieve a reduced-order model of SISO complex linear structures. Also, Du et al. [8] employed a Genetic Algorithm to constrain H_2 model reduction technique intended to MIMO delay models. Fuel cells have become a very large field of research to be a new source of energy for several uses, varying from power generators to mobile applications due to their viability, efficiency and robustness. The proton exchange membrane fuel cell (PEMFC) technology is rapidly being developed. In this work, we want to make a complete assessment and comparison of ANN-BBO based approach and standard BT method for optimal model reduction of PEMFC500w system as a discrete MIMO complex model. Moreover, we consider hybrid (L1, H2 and H∞) criteria of our model reduction problems being studied to get a better compromised reduced model.

2. PEMFC 500W State-space Modelling

The fuel cell output voltage is an important part of its modeling. It is the potential of the cell obtained in an open circuit thermodynamic balance (without load). At normal conditions of pressure and temperature, the Nernst equation of the electrochemical reaction potential$E_{cell}$of one cell is given by [9]:

$$\mathrm{E_{cell}} = E_0^{Cell} + \frac{RT}{2F} ln\left(\frac{P_{H_2}\,(P_{O_2})^{0.5}}{P_{H2O}}\right) \quad (1)$$

where:

E_0 : Reference potential

R : Gas constant (8.3143 J/[mol K])

T : Fuel cell temperature (K)

F : Faraday constant (96487 C/mol)

P_{H_2} : hydrogen pressure (atm)

P_{O_2} : Oxygen pressure (atm)

P_{H2O} : Water pressure (atm)

The open-circuit output voltage of the PEMFC is given as:

$$E_{o.FC} = ns.E_0^{Cell} + ns\frac{RT}{2F}ln\left(\frac{P_{H_2}(P_{O_2})^{0.5}}{P_{H2O}}\right) \quad (2)$$

n_s is the number of cells

The PEMFC dynamics is characterized by non-linear differential equations converted into state-space representation [9]. The net mole flow of oxygen, hydrogen and water at the cathode and at anode correspondingly is given by [10]:

Let : $x_1 = (m_{O_2})_{net}$, $x_2 = (m_{H_2})_{net}$ and $x_3 = (m_{H_2O})_{net}$

$$\dot{x}_1 = \left(\frac{-1}{\lambda_c}\right)x_1 + \left(\frac{1}{4\lambda_c F}\right)I \quad (3)$$

$$\dot{x}_2 = \left(\frac{-1}{\lambda_A}\right)x_2 + \left(\frac{1}{4\lambda_A F}\right)I \quad (4)$$

$$\dot{x}_3 = \left(\frac{-1}{\lambda_C}\right)x_3 + \left(\frac{1}{4\lambda_C F}\right)I \quad (5)$$

The dynamic equations of the partial pressure of hydrogen and oxygen, and the rate of change of the fractional pressure of water is written based on an ideal gas law $P.V = n.R.T$ as [11]:

Let: $x_4 = T$, $x_5 = P_{H_2}$, $x_6 = P_{O_2}$ and $x_7 = P_{H_2O}$

$$\frac{dP_{H_2}}{dt} = \left(\frac{RT}{V_a}\right)(m_{H_2})_{\text{in}} - \left(\frac{RT}{V_a}\right)\cdot(m_{H_2})_{\text{out}} - \left(\frac{RT}{V_a}\right)\frac{I}{2F} \quad (6)$$

Therefore,we have:

$$\dot{x}_5 = 2.\theta_1(x_4)u_{pA} - 2\Theta_1(x_4).x_5 - \Theta_2(x_4).I \quad (7)$$

Where:

$$\Theta_1(x_4) = \left(\frac{R.(m_{H_{2o}}).x_4}{V_a.(P_{H2O})}\right)\theta_2(x_4) = \left(\frac{R_{x_4}}{2V_a F}\right)$$

Similarly, the partial pressure of oxygen dynamic equation can expressed as: $ns.E_0^{Cell}$

$$\dot{x}_6 = 2.\theta_3(x_4)u_{pc} - 2\Theta_3(x_4).x_6 - \Theta_4(x_4).I \quad (8)$$

Where:

$$\Theta_3(x_4) = \left(\frac{R.\left(m_{H_{2o}}\right)_m^c.\ x_4}{V_c.(P_{H2O})_m^c}\right)\theta_4(x_4) = \left(\frac{R_{x_4}}{2V_cF}\right)$$

Similarly The rate of water partial pressure variation is given as:

$$\dot{x}_7 = 2.\theta_5(x_7)x_4 + 2\Theta_4(x_4).I \tag{9}$$

Where :

$$\Theta_5(x_7) = \left(\frac{R.\left(m_{H_{2o}}\right)_{in}^c(P_{H2O}^{in} - x_7)}{V_c.(P_{H2O})_n^c}\right)$$

The net raise in the PEMFC temperature of the assembly is given by:

$$\dot{x}_4 = \frac{1}{M_{fc}C_{fc}}(\dot{x}_8 - \dot{x}_9 - \dot{x}_{10}) \tag{10}$$

Where: M_{fc} is Total mass of PEMFC stack (kg)

C_{fc} is Specific heat capacity of PEMFC stack *[J/(mole.K)]*

$$\dot{x}_8 = \theta_6(x_4, x_5, x_6, x_7).I \tag{11}$$

Where:

$$\theta_6(x_4, x_5, x_6, x_7) = [ns\frac{\Delta G^0}{2F} - \frac{nsRx_4}{2F}ln\left(\frac{x_5.x_6^{0.5}}{x_7}\right)$$

$$\dot{x}_9 = \theta_7(x_4, x_5, x_6, x_7).I \tag{12}$$

With I is stuck current:

$$\theta_7(x_4, x_5, x_6, x_7) = n_s[E_0^{Cell} + \frac{Rx_4}{2F}ln(\frac{x_5.x_6^{0.5}}{x_7}) - V^{Act} - V^{Conc} - V^0]$$

$$\dot{x}_{10} = [h_s n_s A_s].x_4 - [h_s n_s A_s].u_{TR} \tag{13}$$

Replacing equations (2.11), (2.12) and (2.13) into equation (2.10), we can get :

$$\dot{x}_{11} = [\frac{-h_s n_s A_s}{M_{fc}C_{fc}}].x_4 - \theta_7(x_4, x_5, x_6, x_7)\mathrm{I} + \left[\frac{-h_s n_s A_s}{M_{fc}C_{fc}}\right].u_{TR} \tag{14}$$

Where: $\theta_8(x_4, x_5, x_6, x_7) = n_s[\frac{2}{M_{fc}C_{fc}}E_0^{Cell} + \frac{Rx_4}{FM_{fc}C_{fc}}ln(\frac{x_5.x_6^{0.5}}{x_7}) - V^{Act} - V^{Conc} - V^0]$

In general, the state space model of the PEMFC system is given as:

$$\begin{cases} \dot{x}\ (t) = A(\theta).x(t) + B(\theta).u(t) + K(\theta).w(t) \\ y(t) = C(\theta).x(t) + v(t) \\ x_0(t) = x_0 \end{cases} \tag{15}$$

$\dot{x}(t)$are states of system, *u(t)* and *y(t)* are input, output of system correspondingly, *w(t)* is the disturbance input, *v(t)* is the measurement noise, *A* the state matrix, *B* the input matrix, *C* the output matrix and *K* the disturbance matrix.

3. PEMFC ARX -ANN Modelling

For modeling the nonlinear states equations of a PEM500W fuel cell using ANN, we propose an identification approach for identifying dynamic system model from measured input-output data. To represent nonlinear system dynamics, we can estimate nonlinear autoregressive exogenous (ARX) models with tree-partition network. ARX models describe nonlinear structures using a parallel combination of nonlinear and linear blocks [12]. The nonlinear and linear functions are expressed in terms of variables called regressors. Several nonlinear estimators can be used such as wavelet network, sigmoid network, tree partition, custom network, and neural network. In this study, the performance of tree partition estimators is chosen due to the simplicity of its structure.

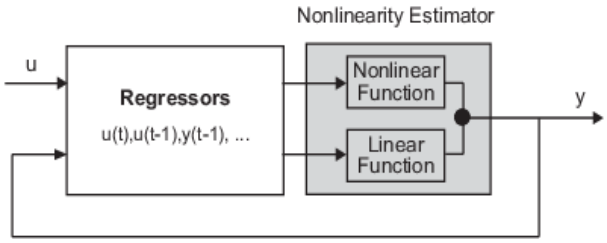

Figure 1. Structure of Nonlinear ARX Models

The output of the nonlinear model was computed by regressor values from the past and current input and past output data such as *u(t),u(t-1),…y(t),y(t-1)*. In Figure 1, the block of nonlinearity estimator can include linear and nonlinear blocks in parallel as:

$$F(x) = L^T(x - r) + d + g(Q(x - r)) \tag{16}$$

Where *x* is the regression vector, *r* is the mean of the regressor *x*. $(L^T(x) + d)$ is the block linear function output and *d* is a scalar offset. $g\big(Q(x - r)\big)$ represents the output of the nonlinear function block. *Q* is a projection matrix that makes the calculations well conditioned. The exact form of *F*(*x*) depends on the choice of the nonlinearity estimator.

4. Optimal hybrid (L_1, H_2, H_∞) norms-based model reduction

4.1 Problem statement

The purpose of model order reduction is to replace a large model by a smaller one, which preserves the essential behavior of the original model. For the systems considered in this work, it can be stated as follows: we have a state space model with identifiable coefficients (a disturbance element) given by the matrix *K* with initial state values given by the vector *x0* and with sample time *Ts*.

The discrete time state-space model of a system with input vector *u*, output vector *y*, and disturbance *e* takes the following equation [13]:

$$\sum_{\mathrm{N}}: \begin{cases} x_N(k+1) = A_N x(k) + B_N u(k) + K_N e(k) \\ y(k) = C_N x(k) + Du(k) + e(k) \\ x(o) = x0 \end{cases} \tag{17}$$

Where $\mathrm{A_N} \in \mathbb{K}^{\mathrm{N}\times\mathrm{N}}$is the state matrix, $\mathrm{B_N} \in \mathbb{K}^{\mathrm{N}\times\mathrm{m}}$, $\mathrm{C_N} \in \mathbb{K}^{\mathrm{p}\times\mathrm{N}}$ and $\mathrm{K_N} \in \mathbb{K}^{\mathrm{N}\times\mathrm{m}}$. The vectors $x(k) \in \mathbb{K}^{\mathrm{N}}$, $u(k) \in \mathbb{K}^{\mathrm{m}}$ and $y(k) \in \mathbb{K}^{\mathrm{p}}$ represent the state, the input and the output of the discrete-time dynamical system, respectively. Often, the order N of the system is too big for solving various control, simulationand optimization problems. The aim of model order reduction is toconstruct a reduced order system:

$$\sum_{\mathrm{n}}: \begin{cases} x_n(k+1) = A_n x(k) + B_n u(k) + K_n e(k) \\ y(k) = C_n x(k) + Du(k) + e(k) \\ x(o) = x0 \end{cases} \tag{18}$$

Where $\mathrm{A}_n \in \mathbb{K}^{n\times n}$, $\mathrm{B}_n \in \mathbb{K}^{n\times m}$, $\mathrm{K}_n \in \mathbb{K}^{n\times m}$, $\mathrm{C}_n \in \mathbb{K}^{\mathrm{p}\times\mathrm{n}}$ and $n \ll \mathrm{N}$,

The quality of this estimation is measured by the error between original system and reduced order system, i.e.:

$$\|\sum_{\mathrm{N}} - \sum_n\| < \varepsilon \tag{19}$$

For a specified precision and a appropriate norm.

4.2 Biogeography Based Optimization (BBO)

The biogeography based optimization (BBO) Algorithm is a new evolutionary algorithm originated by biogeography. As its name involves, the BBO algorithm has been inspired by biogeography [14-20]. The BBO algorithm imitates relations linking diverse types (habitants) situated in diverse habitats in terms of migration, evacuation, and transformation. In reality, this algorithm reproduces the progress of environment, considering movement and transformation among diverse physically alienated areas towards a stable state.

Commonly talking, the ideas of the explore procedure of BBO are the same to those of further evolutionary algorithms, in which a set of arbitrary solutions is initially created. Subsequently, the

primary arbitrary solutions are assessed through a fitness function and after that progresses over a predefined number of iterations. The BBO algorithm is extremely like GA. Exploration agents in BBO, labeled habitats, work equally to chromosomes in GA.

These regulation habitats, labeled habitants, are comparable to genes in GA. The related fitness cost for every habitat in BBO is called the Habitat Suitability Index (HSI). Depending on the HSI of habitats, the habitants are capable to travel starting from a location to another one. In other terms, habitats can progress based on their HSI as:

1. Habitants existing in habitats with elevated HSI are further probable to immigrate to habitats with small HSI.
2. Habitants situated in low-HSI habitats are further flat to let movement of new habitants from habitats with high HSI.

In the BBO algorithm, every habitat is given three rates: immigration (λk), emigration (μk), and mutation. These rates are determined based on the number of habitants as below:

$$\mu_k = \frac{E \times n}{N} \lambda_k = I \times \frac{1-n}{N}$$

Where *n* is the habitant number, *N* is the highest amount of habitants, *E* is the greatest emigration speed, and *I* designates the greatest immigration speed. Figure.2 shows emigration and immigration rates. It demonstrates that the probability of emigration is in relation with the number of habitats. Also, the immigration probability is inversely relative to the number of habitants. The mutation rate of BBO is furthermore a function of the number of habitants and given by:

$$m_n = M \times \left(1 - \frac{p_n}{p_{max}}\right) \quad (20)$$

Where *M* is an initial value for mutation defined by the user, *pn* is the mutation probability of the *n*-th habitat, and pmax=arg max(pn), n=1,2,…,N and pmax=arg max(pn), n=1,2,…,N.

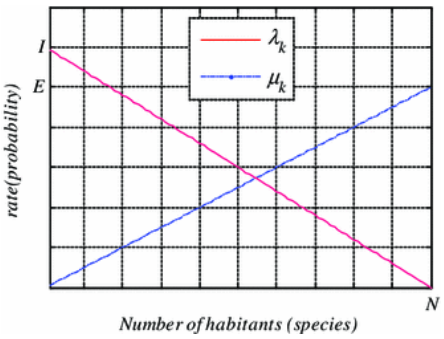

Figure 2. Emigration (μk) and immigration (λk) curves

To resume, the BBO algorithm can be presented as follows:

1. Define the migration probability and mutation probability;
2. population initialization;
3. R_i and R_e calculation of all candidate through the population;
4. Modification of the selected islands based on the immigration rate;
5. Choice of the island from which the *HSI* is to be emigrated based on the emigration rate.
6. Randomly select an *HSI* from the chosen island at step5.
7. Mutation based on each island mutation probability;
8. The objective function computation for each individual island. If the objective function is not fulfilled, go to step three.

4.3 BBO based model order reduction

In this paper, PEMFC500w model reduction problem is investigated using BBO Algorithm, minimizing the hybrid (L_1, H_2, H_∞) norm.

$$\text{Let:} \quad E(z) = G_N(z) - G_n(z) \tag{21}$$

Using different norms leads to diverse approximations since diverse norms desire diverse characteristics of the system. Though, it is sometimes attractive to get a decreased order model by means of some attractive characteristics that might not be attainable through using a particular norm only. Hence, we propose the next hybrid norm condition to get improved compromised reduced order models [21]:

$$\|E\|_{hybrid} = \alpha \|E\|_2 + \beta\|E\|_\infty + \gamma\|E\|_{L1} \tag{22}$$

where ,β and γ are constants

Then the H_2 norm is defined as:

$$\|E\|_2 = \left\{\frac{1}{2\pi}\sum_1^\infty |E(k)|^2\right\}^{1/2} \tag{23}$$

And theH_∞ norm is defined as:

$$\|E\|_\infty = \max|E(k)| \tag{24}$$

The H_{L1} norm is given by:

$$\|e\|_{L1} = \sum_0^\infty |y_N(k) - y_n(k)| \tag{25}$$

Where *e(k)* is the impulse response difference between the original system and the reduced system:

$$e(k) = y(k) - y_n(k) \tag{26}$$

5. Simulation Results

The parameters of the used PEMFC model are specified in the following Table 1. A nonlinear state space model of the PEMFC, developed previously, is simulated in MATLAB software.

Table 1. Parameters of the PEMFC Model [10]

$A_s = 3.2.10^{-2}$ m^2	$M_f = 44$ kg
$a = -3.0810^{-3}$ V/K	$(m_{H_2O})_{in}^{a} = 8.614.10^{-5}$ mol/s
$a_0 = 1.3697$ V	$(m_{H_2O})_{in}^{c} = 8.614.10^{-5}$ mol/s
$b = 9.72410^{-5}$ V/K	$n_s = 48$
$C_k = 500$ J(moLK)	$(P_{H_2O})_{\text{in}} = 2$ atm
$C = 10$ F	$R = 8.31$ J/(mol/K)
$E_0^{\text{Cell}} = 1.23$ V	$R_c^0 = 0.28\Omega$
$e = 2$	$V_a = 10^{-3}$ m^3
$F = 96487$C/mol	$V_c = 10^{-3}$ m^3
$\Delta G^0 = 2372.10^3$ J/mol	$\lambda_A = 60$ s
$h_s = 37.5$ W/(m^2K)	$\lambda_c = 60$ s
$K_I = 1.87.10^{-3}\Omega$/A	$(P_{H_2O})_{in}^{a} = 1$ atm
$K_T = -237.10^{-3}\Omega/K$	$(P_{H_2O})_{in}^{c} = 1$ atm

In order to find the *V-I* characteristics of the PEMFC, the model is simulated via nonlinear state space equations with input variables: u_{pa}= *60atm* ,u_{pc}= *30atm and* u_T=*308 k* . Figures 3 and 4 show the results close match to simulation results obtained by the experimental results of the *Avista Labs SR-12* (500W) PEMFC stack in [11]. The output voltage response of the PEMFC model is presented in Figure 3. The output voltage diminishes from about 38.43 to 25.88 volts.

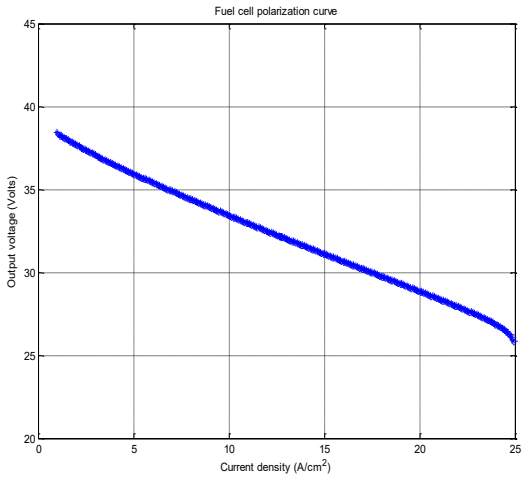

Figure 3. V-I Characteristics of the PEMFC Model

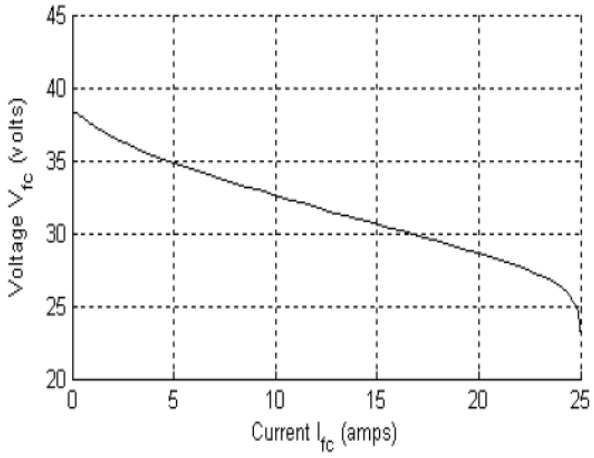

Figure 4. Experimental results of the Avista Labs SR-12 (500W)

The *P-I* characteristics of the PEMFC model are given in Figure 5. The maximum output power is attained at a position near to the rated current of the fuel cell (25A), but not precisely at the rated current. The PEMFC leaves in the concentration area close to the rated current value, where the output power decreases with the rising load current owing to the potential decline in the PEMFC's output voltage**.**

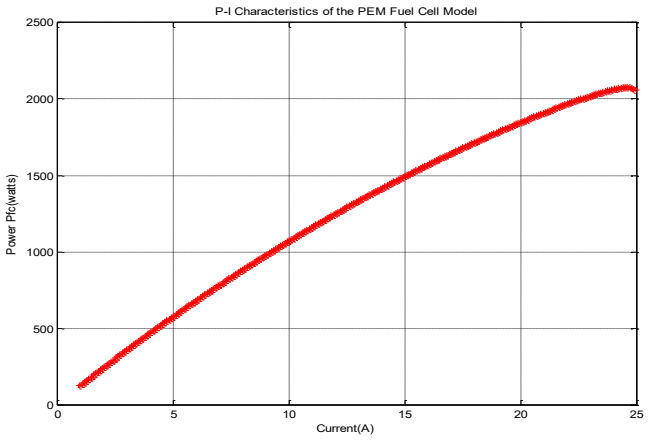

Figure 5. P-I Characteristics of the PEM Fuel Cell Model

After nonlinear equations simulation step of a 500-W proton exchange membrane (PEM) fuel cell, in order to get the voltage and current outputs, we identifieda dynamic system model from measured input-output data using nonlinear ARX models with tree-partition network.Then we linearizethis model to get a state space model with identifiable coefficients (a disturbance element) given by the matrix *K* with initial state values given by the vector *X* and with sample time *Ts =0.2*.

$$Ad = \begin{bmatrix} 0.9004 & 0 & -0.2470 & 0 & -0.5076 & -0.5076 & 0.3498 & 0.3498 \\ 0.2859 & 0 & -0.4406 & 0 & 1.1560 & 1.1560 & -0.7268 & -0.7268 \\ 10 & 0 & 0 & 0 & 0 & 0 & 0 & 0 \\ 0 & 1 & 0 & 0 & 0 & 0 & 0 & 0 \\ 0 & 0 & 0 & 0 & 0 & 0 & 0 & 0 \\ 0 & 0 & 0 & 0 & 0 & 0 & 0 & 0 \\ 0 & 0 & 0 & 0 & 10 & 0 & 0 & 0 \\ 0 & 0 & 0 & 0 & 0 & 10 & 0 & 0 \end{bmatrix}$$

Bd = [0 0; 0 0; 0 0; 0 1; 0 0; 1; 0 0; 0];

Cd = [0.9004 0 -0.2470 0 -0.5076 -0.5076 0.3498 0.3498;
0.2859 0 -0.4406 0 1.1560 1.1560 -0.7268 -0.7268]

Dd = [0 0; 0 0]

Kd = [1 0; 0 1; 0 0; 0; 0 0; 0; 0 0; 0 0; 0]

Xd = [0; 0; 0; 0; 0; 0; 0; 0]

Eigen values: $\lambda_1 = 0, \lambda_2 = 0, \lambda_{3,4} = 0.4502 \pm 0.2104i, \lambda_5 = 0, \lambda_6 = 0, \lambda_7 = 0, \lambda_8 = 0$

With the parameters of the BBO Algorithm utilized are: population size=100, the initial population of candidate solutions is generated randomly, mutation probability is set to 0.04, the number of nodes HSI is 20, the maximum immigration (λ) and emigration (μ) rates are 0.75 and 0.75. The termination

criterion is a function evaluation limit set at 10^{-20} attained at 600 runs; the temporary population is so that all emigrating variables may initiate from the population that is put at starting of the generation. Hence, the results of (L_1, H2,H_{inf}) hybrid norm model reduction with $\alpha = \beta = \gamma$=1:

Ar = [0.21106 0.044441 0.14361; 1.3189 -0.3388 0.89948; -0.36742 -0.19781 -0.089514]

Br = [0.60513 0.96219; 0.0028169 -0.052779; 0.72425 -0.013944]

Cr = [-0.54119 -0.04784 -0.20932; 1.1679 -0.67317 0.62251]

Dr = [-0.014372 -0.0018601; 0.0086205 -0.011826]

Kr = [0.12484 2.5473; 0.71806 -2.6324; 0.16301 -0.68393]

xr(0) = [3.0308; -1.6829; 0.18331]

Eigenvalues: $\lambda_1 =$ -0.1938, $\lambda_{2,3} = -0.0117 \pm 0.3276i$

Table 2 shows the results comparison of the different the relative norms of model error obtained by ANN-BBO and BT approaches with model order reduction n=3:

Table 2. Comparison of the relative norms of error systems obtained by ANN-BBO and BT approaches

norms	ANN-BBO	BT method
H_2 norm	0.0587	0.0837
H_{inf} norm	0.0493	0.0656
L_1 norm	L_1_Norm(:,:,1) = [0.2862 0.0456]	L_1_Norm(:,:,1) = [0.2282 0.0786] L_1_Norm(:,:,2) = 0.2282 0.0786]
(L1, H2, Hinf) hybrid norm	L_1_Norm(:,:,2) = [0.2306 hybrid norm(:,:,1) = [0.3942 0.1536] hybrid norm (:,:,2) = [0.3385 0.1626]	hybrid norm (:,:,1) = [0.3776 0.2279] hybrid norm(:,:,2) = [0.3776 0.2279]

To better evaluate the quality of approximants, we trace the temporal responses in Figures 6-9 blow, and the frequency responses in Figures 10-11 for PEMFC500W original system and the reduced order model by the ANN-BBO approach and BT method of dimension n=3.

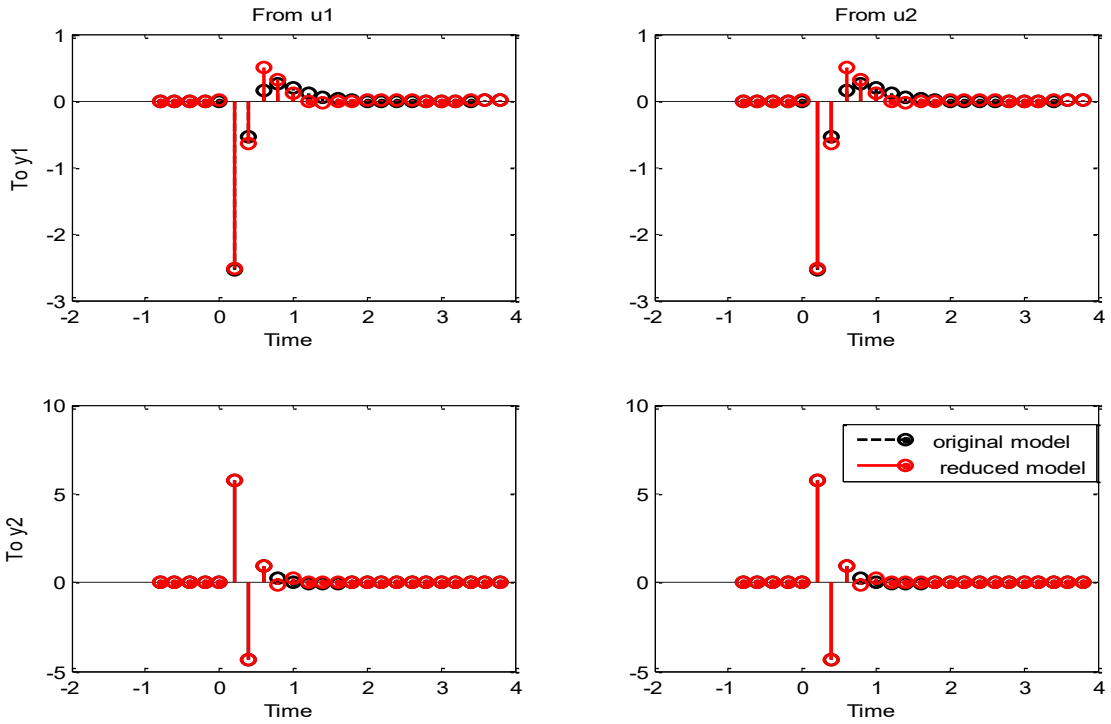

Figure 6. Impulse response by BT approach

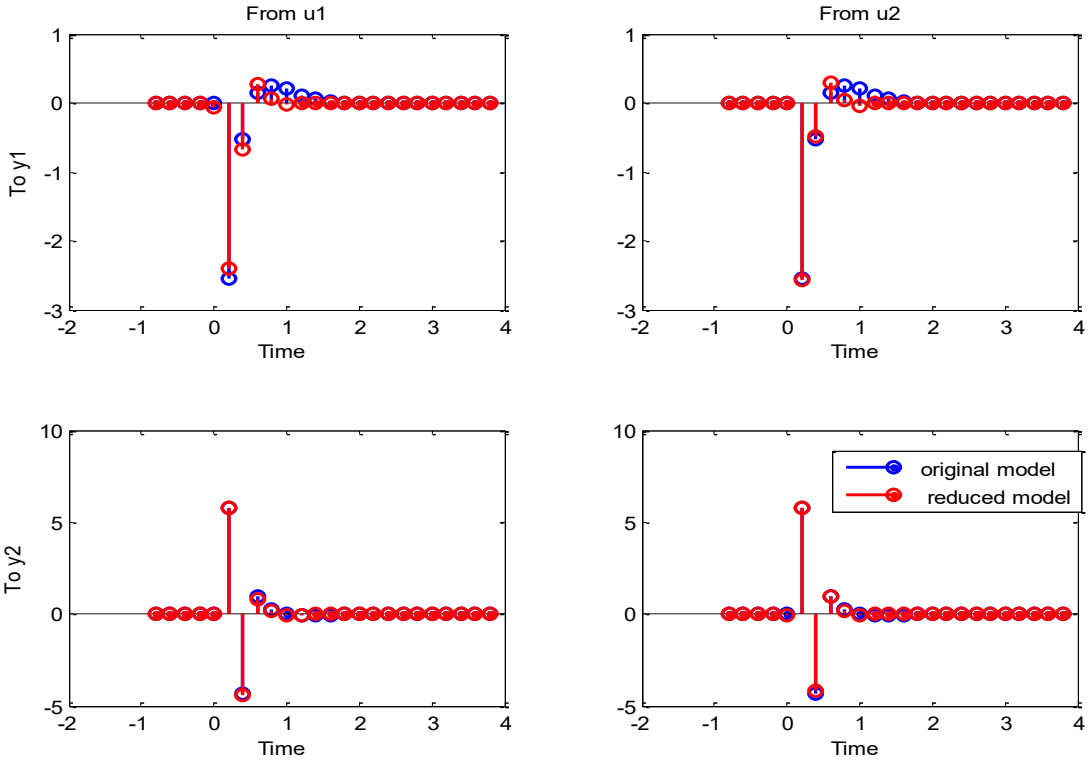

Figure 7. Impulse response by ANN-BBO approach

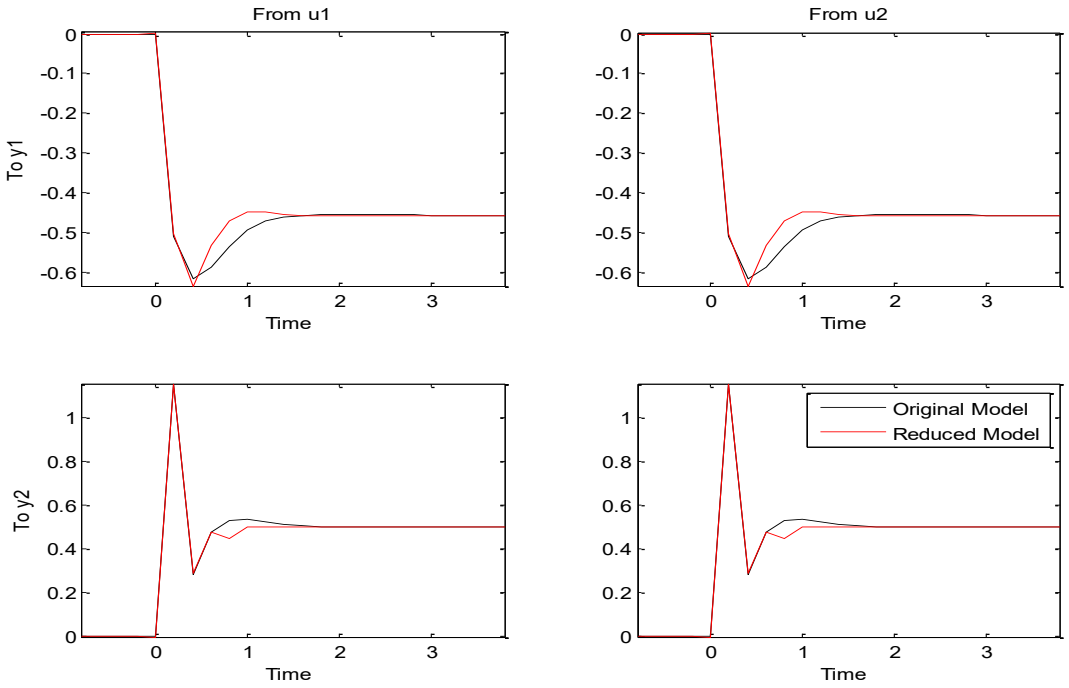

Figure 8. Step response by BT approach

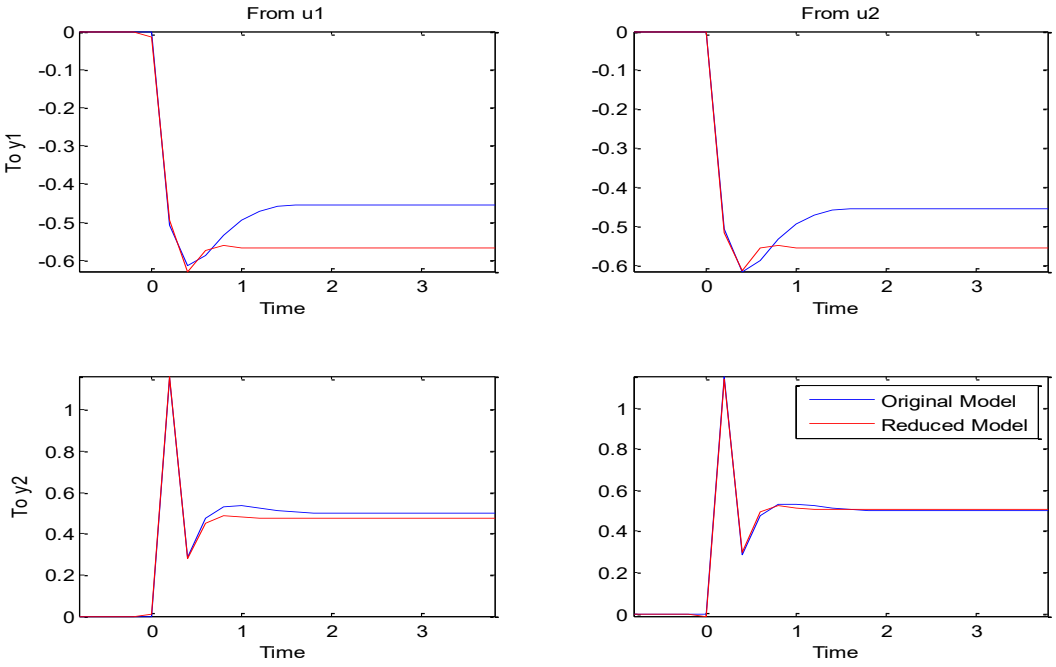

Figure 9. Step response by ANN-BBO approach

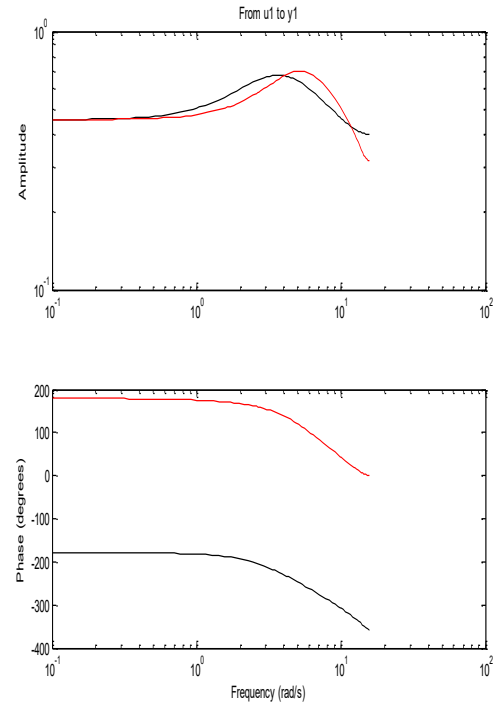

From u1 to y1

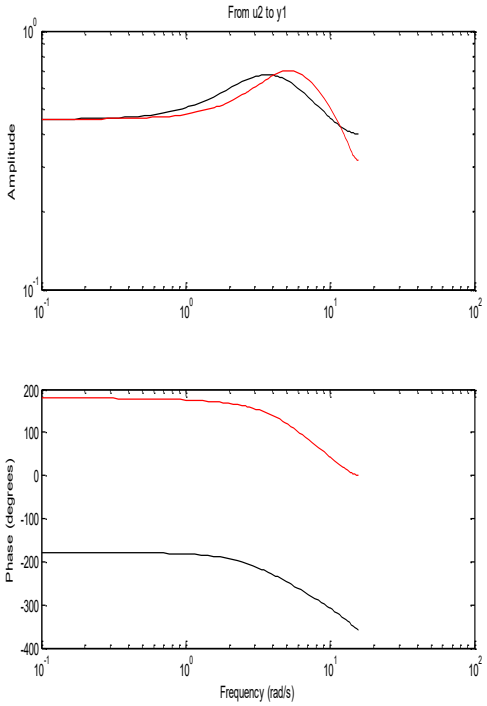

From u2 to y1

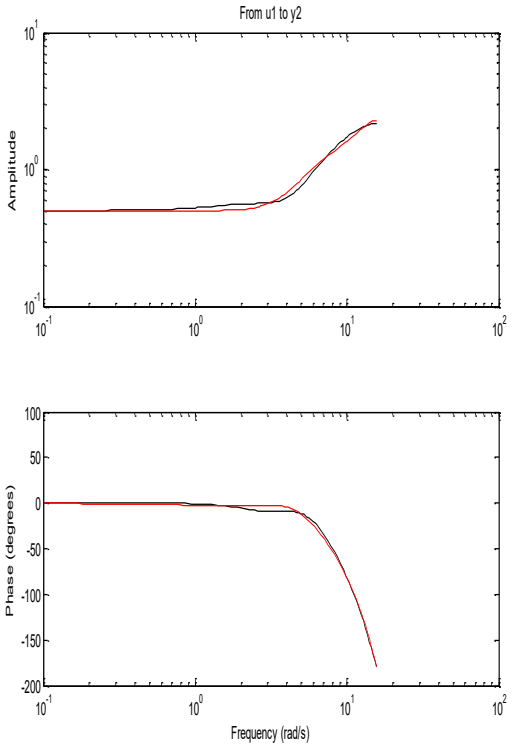

From u1 to y2

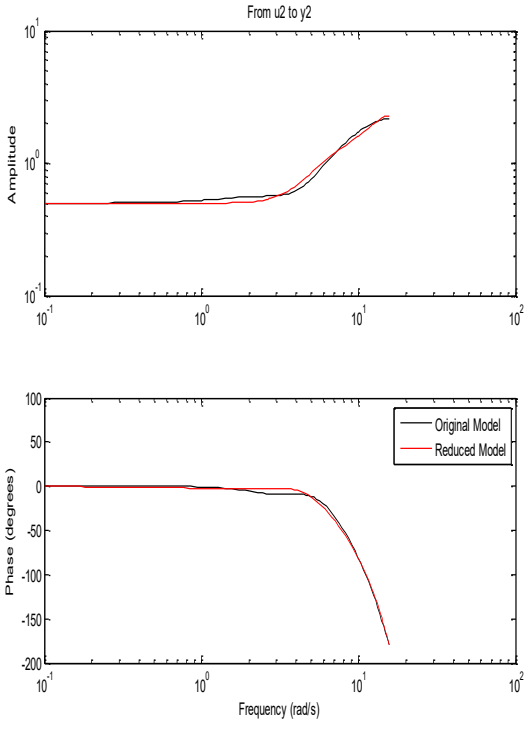

From u2 to y2

Figure 10. Frequency response by BT approach

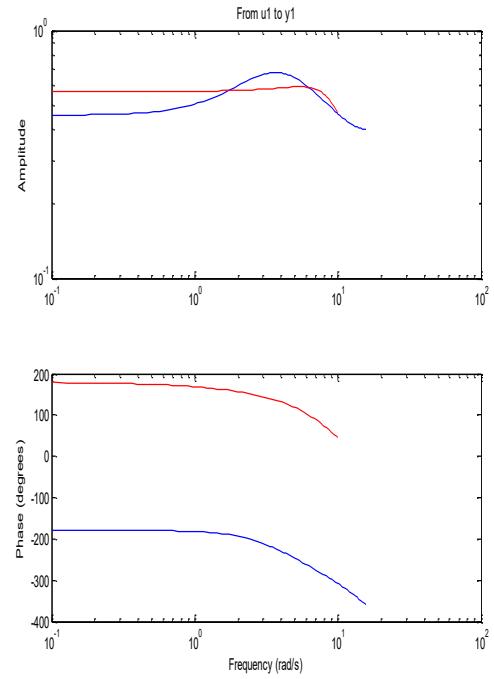

From u1 to y1

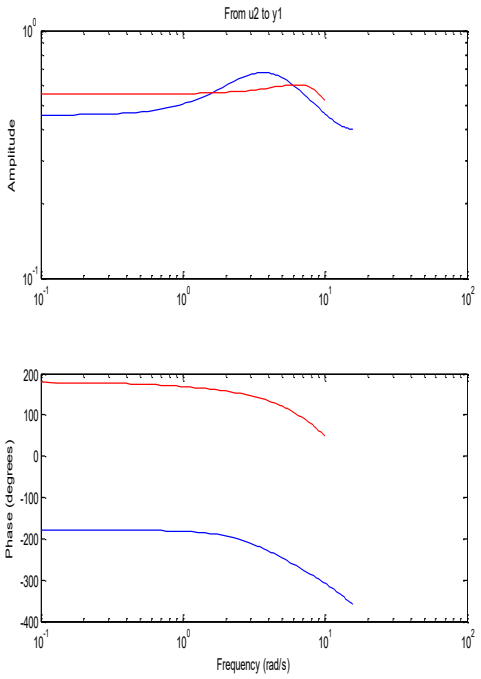

From u2 to y1

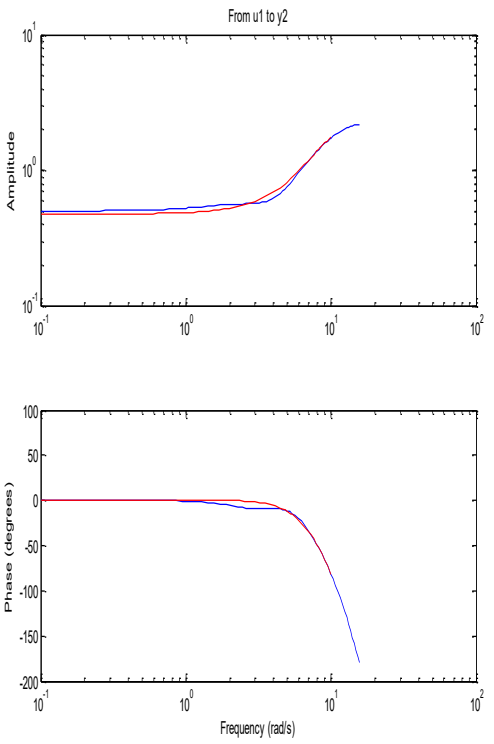

From u1 to y2

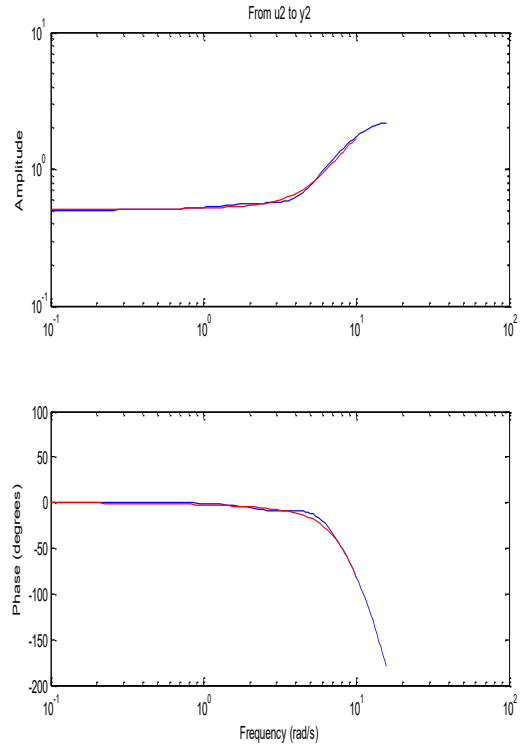

From u2 to y2

Figure 11. Frequency response by ANN-BBO approach

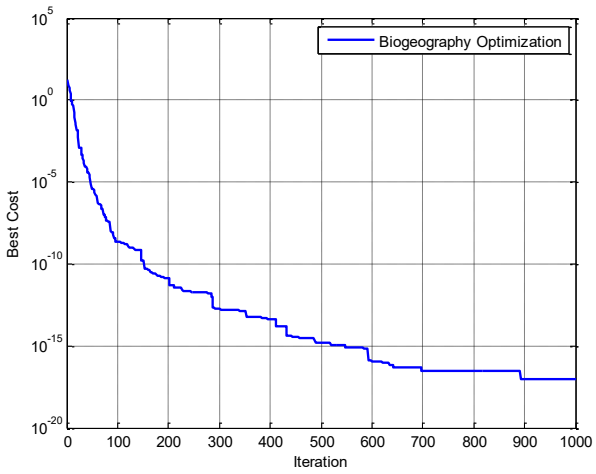

Figure 12. Objective function evolution with runs

We observe in Table.2 that the relative error norms of H_2-norm and H_{inf} - norm systems obtained by ANN-BBO approach are better than those obtained by BT method. But results are different in cases: L_1-norm and hybrid (L_1,H_2, H_{inf}) norms, in which, we find BT method in first output with inputs of hydrogen and oxygen pressures better than ANN-BBO approach. In the contrary, results in the second output show better performance of ANN-BBO approach compared to BT method.

Figures. 6–11 illustrate the impulse responses, step responses and frequency responses of all models, correspondingly. Notice that the impulse responses of the reduced-order model via ANN-BBO is greatly close to those of the original model than using BT method for all outputs. While in step responses, the first output of the reduced-order model by BT method match those of the original model than ANN-BBO approach. The frequency response comportment of the reduced-order model by BT method strictly look like that of the original model than ANN-BBO approach with a little error at elevated frequencies. On the other hand, because the majority of physical systems function at low frequencies, this elevated frequency error can be unobserved. Evolution of system error represented by an objective function minimized by BBO algorithm is illustrated in Figure 12.

6. Conclusion

We have studied in this paper an optimal order reduction of complex MIMO nonlinear dynamic model of PEMFC via (L_1, H_2, H_∞) norms synergy optimized with biogeography based optimization (BBO) Algorithm. The system is modeled using an autoregressive (ARX) model simulated by an artificial neural network (ANN). A comparison is accomplished among BT approach. The results shows us the use of this novel optimal approach in models reduction to the best solution. But it has one drawback

found in its long time achieving the best solution or optimum solution compared to BT approach. The future goal is to realize this optimal controller in hardware implementation. Then, interface to a DC/AC converter for our laboratory research experiments.

References

[1] E.J. Davison, "A Method for Simplifying Linear Dynamic Systems", IEEE. Transaction on Automatic Control, vol. AC-11, pp.93-101, January 1966.
[2] B.C. Moore, "Principal Component Analysis in Linear Systems: Controllability, Observability and Model Reduction", IEEE Transaction on Automatic Control,vol. AC-26, pp. 17-32, 1981.
[3] D.A. Wilson, "Optimal Solution of Model Reduction Problem", Proc. IEE, vol. 117, June 1970.
[4] D.A. Wilson, "Model Reduction for Multivariable Systems", Int. J. Contr., vol. 20, pp.57-64, 1974.
[5] S. Gugercin , A. C. Antoulas , C. Beattie " A Rational Krylov Iteration for optimal H2 model reduction ",
Proceedings of the 17the international Symposium on Mathematical Theory of Network and Systems,Kyoto,Japan, july 24-28,2006
[6] A. Bunse-Gerstner , D. Kubalinska, G. Vossen, D. Wilczek, " h2-norm optimal model reduction for large scale discrete dynamical MIMO systems", Journal of Computational and Applied Mathematics 233 (2010) 1202_1216.
[7] S. Panda, J.S. Yadav, N.P. Padidar, and C. Ardil," Evolutionary Techniques for Model Order Reduction of Large Scale Linear Systems", World Academy of Science, Engineering and Technology International Journal of Electrical and Computer Engineering Vol:6, No:9, 2012
[8]H. Du, J. Lam and B. Huang, "Constrained H2 Approximation of Multiple Input–Output Delay Systems Using Genetic Algorithm", ISA Transaction, vol.46, no. 2, pp. 211-221, March 2007.
[9] A. Haddad, R.Bouyekhf, A. El Moudni, M.Wack, "Non-linear dynamic modeling of proton exchange membrane fuel cell", Journal of Power Sources 163 (2006) 420–432.
[10] SachinPuranik, M.S. "Control of fuel cell based green energy systems for distributed generation application", dissertation presented in Partial Fulfillment of the Requirements for the Degree Doctor of Philosophy in the Graduate School of The Ohio State University 2009.
[11] Caisheng Wang, Nehrir, M.H., Shaw S.R., "Dynamic Models and Model Validation for PEM Fuel Cells Using Electrical Circuits", IEEE Transactions on Energy Conversion, Vol. 20, Issue 2, pp. 442-451, June 2005.
[12] M. A. Ayob, W.N.W. Zakaria, "Estimation of Nonlinear ARX Model for Soft Tissue by Wavenet and Sigmoid Estimators ",ISSN: 2180-1843 e-ISSN: 2289-8131 Vol. 8 No. 7, January 2016.
[13]L.Ljung, "Sytem Identification Toolbox", User's Guide R2015 a . www.mathworks.com
[14] Dan Simon, Biogeography-Based Optimization, IEEE Transactions on Evolutionary Computation (Volume: 12, Issue: 6, Dec. 2008), Page(s):702–713,DOI:10.1109/TEVC.2008.919004.
[15] Chennana, A., Megherbi, A. C., Bessous, N., Sbaa, S., Teta, A., Belabbaci, E. O., ... & Agajie, T. F. (2025). Vibration signal analysis for rolling bearings faults diagnosis based on deep-shallow features fusion. *Scientific Reports*, *15*(1), 9270.
[16] Bentegri, H., Rabehi, M., Kherfane, S., Nahool, T. A., Rabehi, A., Guermoui, M., ... & El-Kenawy, E. S. M. (2025). Assessment of compressive strength of eco-concrete reinforced using machine learning tools. *Scientific Reports*, *15*(1), 5017.

[17] Mehallou, A., M'hamdi, B., Amari, A., Teguar, M., Rabehi, A., Guermoui, M., ... & Khafaga, D. S. (2025). Optimal multiobjective design of an autonomous hybrid renewable energy system in the Adrar Region, Algeria. *Scientific Reports*, *15*(1), 4173.
[18] Tibermacine, A., Akrour, D., Khamar, R., Tibermacine, I. E., & Rabehi, A. (2024, December). Comparative Analysis of SVM and CNN Classifiers for EEG Signal Classification in Response to Different Auditory Stimuli. In *2024 International Conference on Telecommunications and Intelligent Systems (ICTIS)* (pp. 1-8). IEEE.
[19] Mostefaoui, M., Belfedhal, A. E., Larbi, A. A., Rabehi, A., Abderrezzaq, Z., & Dabou, R. (2024, December). Enhanced Detection of EVA Discoloration Defects in Solar Cells Using Vision Transformers and Contrastive Learning. In *2024 International Conference on Telecommunications and Intelligent Systems (ICTIS)* (pp. 1-6). IEEE.
[20] Tibermacine, A., Tibermacine, I. E., Zouai, M., & Rabehi, A. (2024, December). EEG Classification Using Contrastive Learning and Riemannian Tangent Space Representations. In *2024 International Conference on Telecommunications and Intelligent Systems (ICTIS)* (pp. 1-7). IEEE.
[21] R. Salim, M. Bettayeb , "H2 and Hinf optimal model reduction using genetic algorithms", Electrical and Computer Engineering Department, University of Sharjah, P.O. Box 27272, Sharjah, UAE.